

Use of Nitrogen-Implanted Chromium Overcoat for Improving the Durability of Thin-Film Magnetic Media

D.E. Muller, K.C. Walter, K. Sridharan, J.R. Conrad, and S. Agarwal

A feasibility study of the use of nitrogen-implanted chromium as a protective overcoat for thin-film magnetic media was undertaken. Computer hard disks that were pre-sputtered with chromium were implanted with nitrogen using the plasma source ion implantation (PSII) process to produce a chromium nitride containing layer approximately 25 nm thick. Elemental concentration-depth profiles were determined with a scanning Auger microprobe. The presence of chromium nitride in the implanted layer was verified by examination of the broad scan of the Auger spectra. The durability of the PSII-treated hard disks relative to those with a standard carbon overcoat has been characterized with nanohardness, pin-on-disk and thin-film head-on-disk wear tests. A vibrating sample magnetometer was used to evaluate the magnetic properties of the disks. It has been demonstrated that PSII processing has the potential to improve the durability of hard disks without any significant reduction in the magnetic properties.

1. Introduction

THE widespread use of computer technology has placed increasing demands on computer hardware manufacturers to produce hard drives that last longer, store more information, but remain small and lightweight.^[1-4] A general approach to improve hard drive lifetime is to deposit a thin, wear-resistant overcoat on the thin-film magnetic media (hard disks) used in hard drives. A schematic illustration of the typical multilayered makeup of a hard disk is shown in Fig. 1. It consists of a NiP-plated aluminum substrate, a chromium underlayer, a chromium-cobalt alloy magnetic layer, a protective carbon overcoat, and a fluorocarbon lubricant film.^[5] Disks are normally textured (mean surface roughness, $R_a = 5$ nm) in a circumferential manner to prevent the read/write head from sticking to the disk and to orient the magnetic media.^[2,6] Disks without texturing ($R_a = 2$ nm) are used to facilitate nanohardness measurements.

During normal operation of a hard drive, the read/write head rides on a cushion of air approximately 0.1 μm above the rotating disk. However, during startup and shutdown of the hard drive, the head contacts the disk. With continued operation, the inherently harder head begins to cause wear on the disk.^[7] To minimize this problem, an ultra-thin (< 40 nm) wear-resistant carbon overcoat (see Fig. 1) is deposited on the surface.^[8] However, it has been reported that the carbon overcoat is susceptible to oxidation, thereby giving rise to an oxidative wear mechanism.^[9-11] Ion implantation offers a possible alternative route for improving the tribological properties of the disks.

Ion implantation is the process of accelerating ions to high velocities and directing them into the near surface region of a material, thereby altering the chemical composition and properties at the surface.^[12] The low processing temperature, absence of interfaces, as well as retention of surface finish and di-

mensional integrity, are recognized as advantages of ion implantation as a surface modification process. In recent years, nitrogen ion implantation has proven effective in improving the wear resistance of engineering materials, tools, and components.^[13-16] The predominant strengthening mechanism is believed to be the formation of hard nitride phase particles at the surface. Therefore, materials containing alloying elements with a high affinity for nitrogen (*e.g.*, chromium), respond particularly well to nitrogen ion implantation.^[17]

A cost-effective approach to ion implantation, plasma source ion implantation (PSII), has recently been developed.^[18-20] Here, targets to be implanted are placed in the plasma source and pulse-biased to a high negative potential. A plasma sheath forms around the target, accelerating ions toward the target and normal to the target surface, thereby implanting all surfaces uniformly. Figure 2 shows a schematic illustration of the PSII process. The cost-effectiveness of PSII compared to conventional beamline implantation stems from two factors: (1) it is inherently a non-line-of-sight process and (2) because the ions impinge on the surface at normal incidence, maximum dose is retained by the target. The effective-

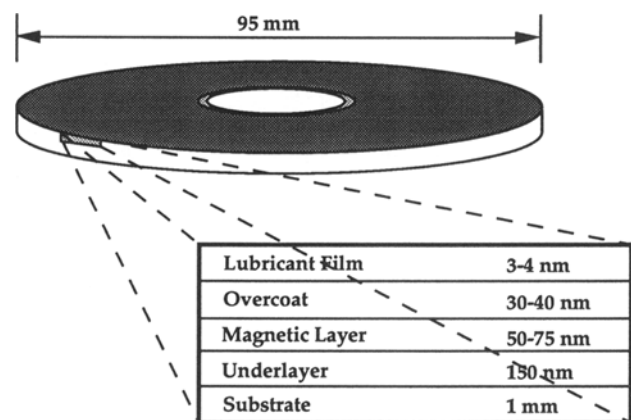


Fig. 1 Cross section of a typical computer hard disk showing the multilayered makeup and the approximate thickness of each layer.

D.E. Muller, Department of Materials Science and Engineering; K.C. Walter, K. Sridharan, and J.R. Conrad, Engineering Research Center for Plasma Aided Manufacturing, the University of Wisconsin, Madison, Wisconsin. S. Agarwal, Akashic Memories Corporation, San Jose, California.

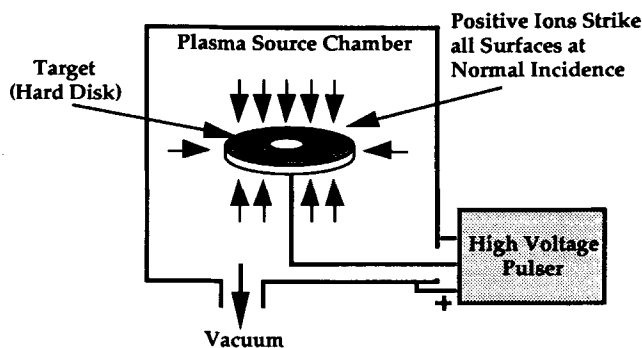


Fig. 2 Schematic of the plasma source ion implantation process.

ness of PSII in improving the wear resistance of a wide variety of engineering materials has been amply demonstrated.^[21]

Recent studies have examined the possibility of hard disk durability improvement through formation of more wear-resistant carbon overlayers produced by various methods including diamond-like carbon (DLC) film by PSII and by compositional variations in the sputtering gas.^[4,22] The purpose of the present investigation is to examine the feasibility of an alternative approach, namely PSII nitrogen ion implantation of hard disks pre-sputtered with a thin layer of chromium.

2. Experimental Procedures

2.1 Plasma Source Ion Implantation Disk Processing

Textured and untextured disks were sputter deposited with a 50 nm chromium layer instead of the traditional carbon overcoat. The disks were mounted on the PSII chamber target stage, and after the chamber was pumped down to a pressure of 10^{-6} torr, they were argon sputter cleaned with a dose of 1×10^{16} ions/cm² to remove the chromium oxide layer on the surface. The disks were then implanted with nitrogen to a dose of 2×10^{17} ions/cm² at a target bias of 8 keV and an operating pressure of 10^{-4} torr. The disks were not lubricated after implantation, and all analyses reported in this investigation pertain to unlubricated disks.

The conditions for sputtering and implantation were determined using the computer simulation, TAMIX (Transport And MIXing from ion irradiation).^[23] This dynamic collisional model predicts the amount of target material lost due to sputtering during implantation, as well as the depth profile of the implanted species. TAMIX simulations for doses of 1×10^{17} , 2×10^{17} , and 3×10^{17} ions/cm² of nitrogen implanted into chromium at a target bias of 8 keV are shown in Fig. 3. As expected, higher doses result in a greater nitrogen concentration at the surface, but the total depth of the implanted layer (largely a function of target bias) does not differ for the three doses tested. However, it is well known that target sputtering increases with dose. In fact, TAMIX predictions show that the surface recession for doses of 1×10^{17} , 2×10^{17} , and 3×10^{17} ions/cm² are 11, 19, and 27 nm, respectively. Because this surface recession is a substantial fraction of the sputtered chromium layer thickness, a dose of 2×10^{17} ions/cm² was selected from the stand-

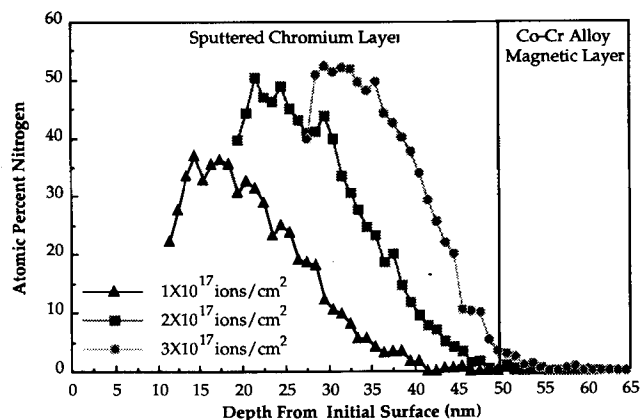


Fig. 3 TAMIX simulation showing the nitrogen concentration profiles in chromium for implantation doses of 1×10^{17} , 2×10^{17} , and 3×10^{17} ions/cm² (target bias, 8 keV).

point of maximizing the nitrogen concentration and minimizing chromium sputtering. For example, at a dose of 3×10^{17} ions/cm², the reduction of the chromium layer thickness due to sputtering would result in the penetration of nitrogen ions into the magnetic layer (see Fig. 3).

2.2 Auger Spectroscopy

The elemental concentration-depth profile was determined with a scanning Auger microprobe. A 1-mm² area of the sample was intermittently sputtered with 3-keV argon ions. After each sputter step, Auger spectra for the specified elements were collected, and the atomic concentration of each element was determined from these spectra. The final depth of the sputtered region as determined by profilometry was used to convert this information to concentration versus depth profiles. The broad scan of the Auger spectra was examined to qualitatively determine the chemical state of chromium in the implanted layer.

2.3 Nanohardness Measurement

A preliminary analysis of the surface mechanical properties was performed using the nanohardness technique.^[24] Here, a current-driven coil and magnet are used to control the force on a tetrahedral diamond-tipped indenter to a resolution of 2.5 μ N to produce an ultra-fine indentation of the sample surface. The indentation depth is determined by a capacitance displacement gage. The hardness in units of GPa is calculated from the projected area of the indentation and the applied force. Nanohardness indentations were made at depths ranging from 15 to 65 nm. Hardness versus depth profiles were determined using data from five indentations at each depth.

2.4 Wear Testing

The pin-on-disk (spherical stylus on a flat sample) configuration wear test was performed to compare the relative wear resistance of untextured disks.^[25] Ruby was used as a stylus material because of its high hardness and chemical inertness. Testing was done with an applied load of 20 g for 30 min. Depths of the wear tracks produced, as measured with a profilometer, were considered to be a measure of wear resistance.

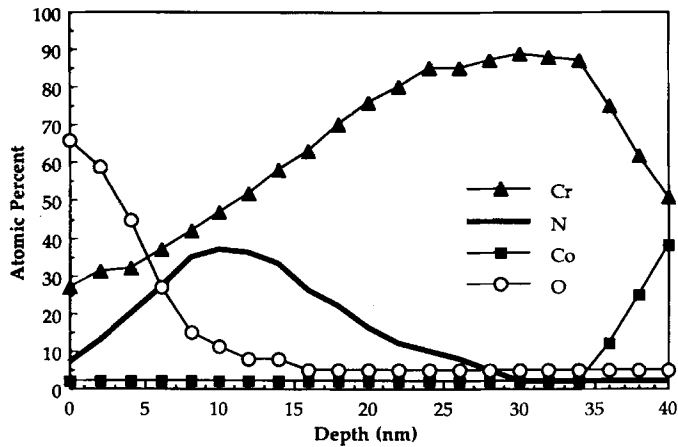


Fig. 4 Elemental concentration-depth profiles as determined by scanning Auger microprobe.

To simulate the wear conditions encountered by a hard disk more effectively, thin-film head-on-disk wear testing was performed on textured disks. Here a two-rail, thin-film head made of a hard $\text{Al}_2\text{O}_3\text{-TiC}$ ceramic composite was placed in sliding contact with the surface of the disk. Testing was done 25 mm from the outer diameter (normal startup/shutdown contact area) using a disk speed of 60 rpm for 30 min. Friction output was recorded with a chart recorder, whereas the level of wear was determined by the number of cycles necessary to reach the maximum level of friction. This wear criteria was used because variations in the surface topography of textured disks makes measurement of the wear track with a profilometer difficult. The loads selected for both wear tests were based on prior experience with overcoats and the actual force exerted by the head on the disk during startup and shutdown procedures.^[2,26]

2.5 Vibrating Sample Magnetometer Measurements

The magnetic properties of the disks were evaluated with a vibrating sample magnetometer (VSM). The VSM test gives an output of the coercivity (H_c) level in units of oersteds (Oe), the magnetization level in electromagnetic mass units (emu), as well as a plot of the hysteresis loop.^[27] This is measured in both the circumferential and radial directions. A reduction in the coercivity level and a departure from the typical square shape of the hysteresis loop in the circumferential direction relate to a reduction in the magnetic storage capacity of the disk.

3. Results and Discussion

The elemental concentration versus depth profiles in the implanted layer is shown in Fig. 4. Typical of the ion implantation process, the nitrogen concentration profile is roughly Gaussian, with a subsurface maximum of ≈ 40 at.% nitrogen occurring at a depth of about 10 nm. The implanted layer thickness was estimated to be 25 nm. The increase in the cobalt concentration shown in Fig. 4 represents the beginning of the magnetic layer. This profile suggests that the TAMIX-predicted implantation parameters were reasonably appropriate because nitro-

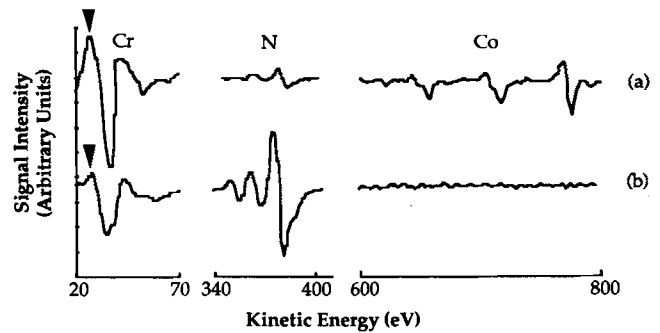


Fig. 5 Broad scan of the Auger spectrum at (a) 40 nm depth showing free chromium and (b) 10 nm depth showing nitrogen-implanted chromium. The expanded versions of the respective 36-eV chromium peaks show the difference in shape of the elbow adjacent to the principal peak (indicated by arrows).

gen did not penetrate the chromium-cobalt alloy layer, which may have adversely affected the magnetic properties. However, the fact that nitrogen did not penetrate the entire thickness of the chromium layer suggests that the implantation parameters could be further optimized by increasing the target bias and/or dose.

The chemical state of chromium was determined by comparing the shapes of the 36-eV energy signals of chromium at depths of approximately 40 and 10 nm using the technique suggested by Singer and Murday.^[28] The broad scan Auger spectra of the relevant elements at depths of 40 and 10 nm are shown in Fig. 5(a) and 5(b), respectively. An expanded version of the 36-eV chromium peak is shown on the left of each spectra. Figure 5(a) shows the spectra of free chromium near the overcoat/magnetic layer interface (note the small nitrogen peaks and emergence of cobalt peaks), whereas Fig. 5(b) shows the spectra of nitrogen-implanted chromium near the peak nitrogen concentration (note the larger nitrogen peaks). The expanded versions of the 36-eV signal clearly show the difference in the shape of the "elbows" adjacent to the principal peak (indicated by arrows). The larger elbow in Fig. 5(a) is indicative of free chromium, whereas the smaller elbow in Fig. 5(b) is indicative of nitrogen bound to chromium in the form of chromium nitride.

The results of the nanohardness characterization are shown in Fig. 6. The data scatter observed is an inherent feature of nanohardness testing and stems from the fine size scale of the indentations, which makes them very sensitive to surface topographical and compositional variations. The data shown in Fig. 6 suggest that nitrogen implantation of chromium increases the hardness of the sputtered chromium overcoat, but the hardness is still lower than that of the carbon overcoat. However, the thicknesses of the overcoats tested, namely chromium (≈ 50 nm), nitrogen-implanted chromium (≈ 25 nm), and the carbon overcoat (≈ 40 nm), are different. Consequently, the hardness data include varying levels of contribution from the multilayered magnetic media substrate,^[22,24] which is softer than the three overcoats tested. The nanohardness data are inconclusive with regard to indicating a significant superiority of either the nitrogen-implanted chromium layer on the carbon overcoat.

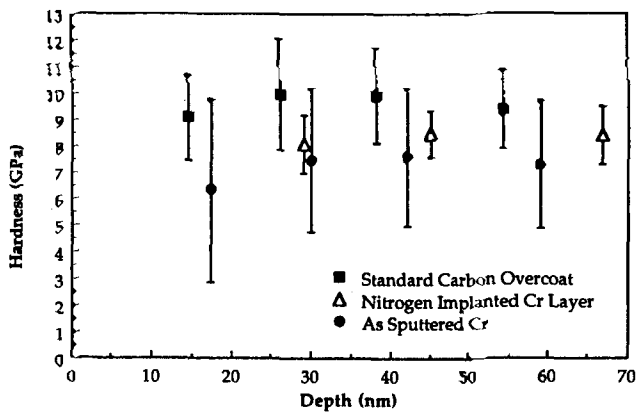


Fig. 6 Nanohardness measurements comparing the standard carbon overcoat, the as-sputtered chromium layer, and the nitrogen-implanted chromium layer.

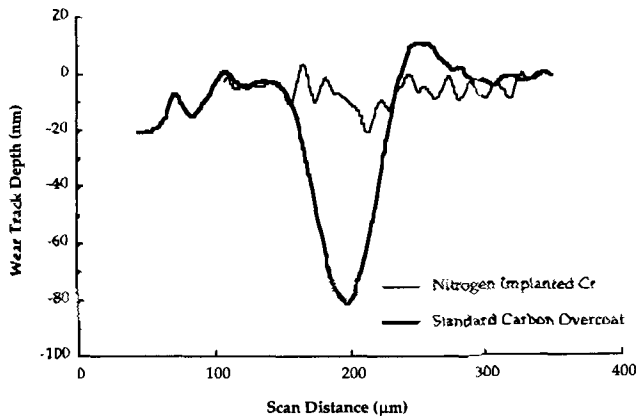


Fig. 7 Typical pin-on-disk wear track profiles of carbon overcoat and nitrogen-implanted chromium layer.

Pin-on-disk wear testing created a visible wear track on the untextured carbon overcoat and nitrogen-implanted chromium disks. The average wear track depths (from eight measurements of each track) are as follows: The carbon overcoat disk is ≈ 80 nm and the nitrogen-implanted chromium disk is ≈ 20 nm. Figure 7 shows the typical wear track profiles of the carbon overcoat and nitrogen-implanted chromium disks, respectively. This wear test indicates a significant improvement in the abrasive wear resistance of the nitrogen-implanted chromium layer over the currently used carbon overcoat. However, it should be noted that the 80 nm wear track depth on the carbon overcoat disk is greater than the depth of the overcoat itself, whereas the 20 nm wear track depth of the nitrogen-implanted chromium disk is very close to the actual layer thickness of 25 nm. Due to the simple contact geometry and to the overriding abrasive wear mechanism, this test provides a comparison of the two different overcoats without the effects of texturing or thin-film head roughness and shape.^[26]

Textured disks with the carbon and nitrogen-implanted chromium overcoats were subjected to the thin-film head-on-disk wear test. The output in volts from the wear tester, as re-

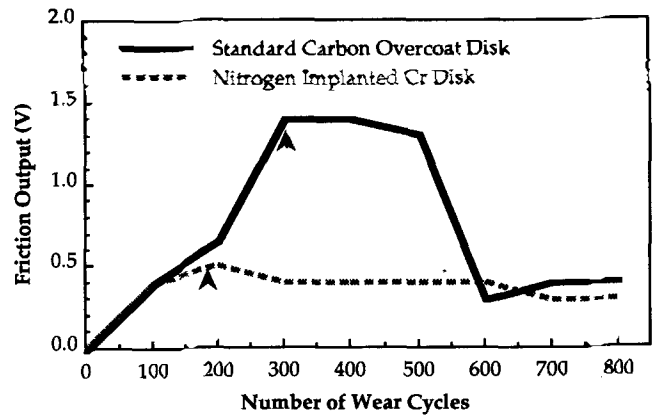


Fig. 8 Thin-film head-on-disk wear testing results showing the friction output for the standard carbon and the nitrogen-implanted chromium overcoats. Arrows indicate the approximate number of wear cycles required to reach the maximum friction level.

corded on a chart recorder, is shown in Fig. 8. This output was taken as a measure of the frictional resistance. The test parameters were identical for both disks, consequently, the friction output shown in Fig. 8 represents a reasonably accurate comparison. The higher output value for the carbon overcoat disk compared to the nitrogen-implanted chromium disk suggests a higher level of friction, but the implanted disk reached the maximum friction level at a slightly lower number of wear cycles (indicated by arrows in Fig. 8). These results show a lower level of friction, but more wear, for the nitrogen-implanted chromium disk compared to the carbon overcoat disk. An important consideration in this test is the effect of texturing, which tends to minimize any wear resistance improvement because of the contribution of wear initiators in the form of head and disk wear debris.

Magnetic property measurements made with the VSM are summarized as follows:

	Coercivity, Oe	
	Circumferential	Radial
Unimplanted side.....	1136	680
Implanted side.....	1152	672

Measured variations of this magnitude in the coercivities of identically processed disks are not unusual; therefore, the differences in the coercivity readings shown above are not statistically significant. The hysteresis loops for the implanted and unimplanted sides of the disk are shown in Fig. 9. Note that there is no significant difference in either the size or shape of the loops. It is clear from these data that the relevant magnetic properties were not adversely affected by the nitrogen on implantation.

4. Conclusions

A new approach involving nitrogen ion implantation of a pre-sputtered chromium layer for improving the wear resis-

tance of thin film magnetic media has been investigated. The implantation resulted in a chromium nitride-containing layer about 25 nm thick. Nanohardness measurements showed that the near surface hardness improved after implantation, but it was somewhat lower than the traditional carbon overcoat. A part of this difference may be attributed to the greater thickness of the carbon overcoat. Pin-on-disk wear testing showed the implanted layer to be superior to the carbon overcoat. Thin-film head-on-disk wear testing indicated that the friction level was lower for the implanted layer, but reached its maximum level of friction at a slightly lower number of wear cycles compared to the carbon overcoat. Finally, the magnetic properties were not affected by the implantation process. This study indicates that nitrogen implantation of a pre-sputtered chromium, along with further optimization of the implantation parameters, may provide a low friction, wear-resistant overcoat for thin-film magnetic media.

Acknowledgments

The authors are grateful to Akashic Memories Corporation, San Jose, CA, for providing the hard disks, use of the thin-film head-on-disk wear tester, and for the vibrating sample magnetometer data. The authors would like to thank R.P. Fetherston and B. Qiu for their assistance in this work. This work was supported by ERC-NSF Grant No. 8721545, U.S. Army Grant No. DAAL02-90-124, and the Minnesota Supercomputer Center Grant No. MG-32804.

References

1. Akashic Memories Corp. Newsletter, 1(3), July (1991).
2. B. Marchon, S. Vierk, N. Heiman, R. Fisher, and M. Khan, *Trib. Mech. Magnetic Storage Systems*, 6, SP-26 STLE, 71 (1989).
3. C.J. Torng, J.M. Sivertsen, J.H. Judy, and C. Chang, *J. Mater. Res.*, 5, 2490 (1990).
4. B. Marchon, P.N. Vo, M.R. Khan, and J.W. Ager, III, *IEEE Trans. Magn.*, 27, 5160 (1991).
5. D. Muller, S. Agarwal, and N. Heiman, unpublished research, Akashic Memories Corp., San Jose, CA (1991).
6. American National Standard Institute, ANSI Standard B46.1 (1978).
7. B. Bhushan, *Tribology and Mechanics of Magnetic Storage Devices*, Springer—Verlag, New York (1990).
8. R.L. White, M.F. Doerner, and G.W. Walker, *Mater. Res. Soc. Symp. Proc.*, 188 (1990).
9. B. Marchon, M.R. Khan, N. Heiman, P. Pereira, and A. Lautie, *IEEE Trans. Magn.*, 26, 2670 (1990).
10. C.J. Torng, J.M. Sivertsen, J.H. Judy, and C. Chang, *J. Mater. Res.*, 5, 2490 (1990).
11. M. Yang, S.K. Ganapathis, R.D. Balanson, and F.E. Talke, *IEEE Trans Magn.*, 27, 5157 (1991).
12. P.D. Townsend, J.C. Kelly, and N.E.W. Hartley, *Ion Implantation and Their Applications*, Academic Press, London (1976).
13. G. Dearnaley, *Thin Solid Films*, 107, 315 (1983).
14. H. Herman, *Nucl. Instrum. Methods*, 182/183, 887 (1981).
15. C. Weist, G.K. Wolf, and P. Ballhause, *Mater. Sci. Eng.*, 90, 399 (1987).
16. P. Sioshansi, *Mater. Sci. Eng.*, 90, 373 (1987).
17. L. Palmethofer, J. Faderal, and F. Lehner, *Mater. Sci. Eng.*, 114, 173 (1989).

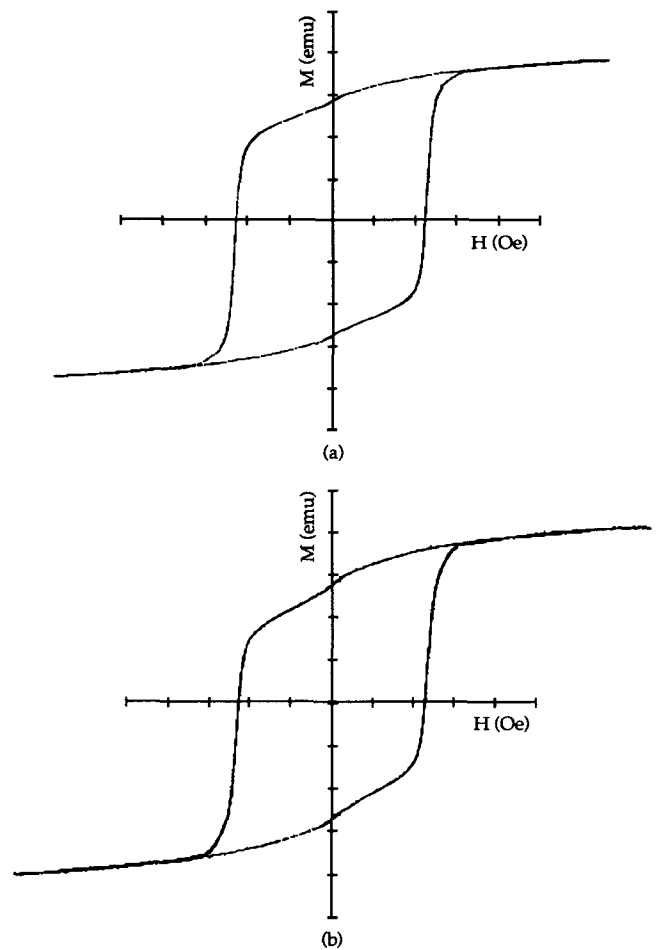


Fig. 9 Vibrating sample magnetometer output showing hysteresis loops in the circumferential direction for (a) untreated chromium side and (b) nitrogen-implanted chromium side of disk. One unit of magnetization (M) = $\times 10^{-3}$ emu; one unit of coercivity (H) = 500 Oe.

18. J.R. Conrad, U.S. Patent No. 4, 764,394, Aug (1988).
19. J.R. Conrad, J.L. Radtke, R.A. Dodd, F.J. Worzala, and N.C. Tran, *J. Appl. Phys.*, 62, 4591 (1987).
20. J.R. Conrad, R.A. Dodd, S. Han, M. Madapura, J. Scheuer, K. Sridharan, and F.J. Worzala, *J. Vac. Sci. Technol.*, 4, 3146 (1990).
21. Engineering Research Center for Plasma-Aided Manufacturing, Annual Report, University of Wisconsin-Madison, June (1991).
22. R. Peters, "Characterization of Thin Amorphous Hydrogenated Carbon Films Produced By Plasma Source Ion Implantation as Protective Coatings on Computer Hard Disks," M.S. thesis, University of Wisconsin-Madison (1991).
23. S.H. Han, G.L. Kulcinski, and J.R. Conrad, *Nucl. Instrum. Methods*, 45, 701 (1990).
24. J.B. Pethica, R. Hutchings, and W.C. Oliver, *Philos. Mag. A*, 48, 593 (1983).
25. A. Chen, X. Qiu, J.R. Conrad, R.A. Dodd, F.J. Worzala, and J. Blanchard, *J. Mater. Eng.*, 12, 299 (1990).
26. M. Chu, B. Bhushan, and L.C. DeJonghe, *Trib. Mech. Magnetic Storage Systems*, 7, SP-29 STLE, 9 (1990).
27. T.C. Arnoldussen, *Proc. IEEE*, 74(11) (1986).
28. I.L. Singer and J.S. Murday, *J. Vac. Sci. Technol.*, 17, 327 (1980).